JOURNAL OF GEOPHYSICAL RESEARCH, VOL. 104, NO. D22, PAGES 27,803-27,810, NOVEMBER 27, 1999

Impact on ECMWF forecasts of changes to the albedo of the boreal forests in the presence of snow

Pedro Viterbo
European Centre for Medium-Range Weather Forecasts (ECMWF), Reading, England

Alan K. Betts
Pittsford, Vermont

Abstract. A change in the calculation of the albedo for the boreal forests in the presence of snow in the European Centre for Medium-Range Weather Forecasts (ECMWF) model, which reduces the deep snow albedo from 0.8 to 0.2, greatly reduces the model systematic cold temperature bias both at the surface and in the lower troposphere at high northern latitudes in the spring.

1. Introduction

For several years the springtime 2-m temperature forecasts from the European Centre for Medium-Range Weather Forecasts (ECMWF) for high northern latitudes have had a systematic cold bias in the presence of snow. It has been suggested by several research groups that the model cannot effectively distinguish snow over bare ground from the snow hidden below the forest canopy. During the April 1996 intensive observation period of the Boreal Ecosystem-Atmosphere Study (BOREAS) in the Canadian boreal forest the ECMWF daytime forecast of near-surface temperatures was 10-15 K colder than observations [*Sellers et al.*, 1997]. A time series of the model albedo, together with the observed and the ECMWF model 36-hour forecast 2-m temperatures for the beginning of April 1996 in the BOREAS southern study area in Saskatchewan, Canada, shown in Figure 1, points directly to the source of the problem. The thick dashed curve is the model forecast temperature at 53.63°N, 106.2°W, the location of the Old Aspen site in the Prince Albert National Park (site data shown as a thin solid curve). The thick solid line is data at the Old Jack Pine site nearby to the northeast at 53.92°N, 104.69°W. At the beginning of April, when there is snow in the model (and on the ground), the model albedo is close to 0.8, and there is a strong cold bias of about 10 K on most days at 0000 UTC, which is at the end of the diurnal heating cycle (1800 LT) for the preceding Julian day. Generally, the coniferous site, which has a lower albedo [*Betts and Ball*, 1997], is warmer than the deciduous aspen site. The times for which the cold bias is less (0000 UTC on April 3, 7, 10) follow cloudy days when the observed diurnal rise of the temperature is small. When the snow "melts" (which happens in the model on April 12, 1996), the forecast albedo decreases to its background value of 0.12, and the forecast temperature becomes much closer to observations.

Some ground truth estimates for the albedo at selected sites are given by *Betts and Ball* [1997], who studied the annual cycle of albedo for 1994 and 1995 at 10 BOREAS measurement sites located over grass, the aspen forest, and the coniferous forests, using data from upward and downward looking pyranometers mounted on towers above the canopy. Representative winter values for daily averaged albedo of snow-covered grass sites are 0.75, while corresponding values for the aspen and conifer sites are 0.21 and 0.13, respectively, with a few values as high as 0.4, 24-48 hours after snowfall. For these two winters, the albedo of the aspen site exceeded 0.3 (and the coniferous sites exceeded 0.2) for about ten 2-day periods, following high snowfall situations. These albedos decreased quickly to the representative winter values after the intercepted snow melts, evaporates, or blows off with the wind. Data from other observational studies in forest areas corroborate these results [*Robinson and Kukla*, 1984; *Harding and Pomeroy*, 1996; *Pomeroy and Dion*, 1996]. The surprisingly few attempts of making a hemispheric-satellite based estimate of albedo [e.g., *Laine and Heikinheimo*, 1996; *Robinson and Kukla*, 1985] suggest lower albedos over the boreal forests than in adjacent grassland areas. However, the absolute values of these satellite estimates might be questionable, because when the surface is snow-covered, it is difficult to distinguish scenes with low cloud and exclude them.

The above evidence suggested that a new treatment of the boreal forest albedo in the presence of snow (hereinafter referred to as the "snow albedo") was necessary in the model: one which effectively distinguishes forest covered and what we shall loosely call "forest-free" areas. This paper describes the changes made to the snow albedo scheme and the extensive experimentation done. In section 2 we outline the old and new snow albedo treatments: some more details are given in the Appendix. Section 3 presents the impact on forecasts in spring, including 2-m temperatures, scores, and systematic errors, and section 4 presents the impact on an ensemble of long runs in spring. This new snow albedo scheme was implemented in the operational model on December 10, 1996. In conclusion, we show the large reduction in the 850 mbar cold temperature bias in the operational ECMWF model over the boreal forest between spring 1996 and spring 1997.

2. Description of Model Changes

2.1. Albedo in Operational Model Before December 1996

The model forecast albedo in a grid box was a combination of the background albedo over a snow-free grid box fraction, with a calculated snow albedo for the remaining snow-covered fraction. In the operational model, prior to December 1996, this snow albedo was done following a fairly complex series of computations, involving background albedo, snow depth, roughness length, vegetation fraction, surface temperature, and interception reservoir contents. However, the end result of these computations was unsatisfactory as it gave an albedo in the presence of snow that is rarely outside of the 0.7- 0.8 range (see Appendix and Figure 3b below). *Betts et al.* [1998] shows that as a result, the net radiation in the model is very low in spring in comparison with observations over the boreal forest. This same paper shows a similar error in the National Centers for Environmental Prediction and National Center for Atmospheric Research (NCEP/NCAR) reanalysis model, which has an albedo for the high-latitude forests near 60%.

Paper number 1998JD200076.
0148-0227/99/1998JD200076$09.00

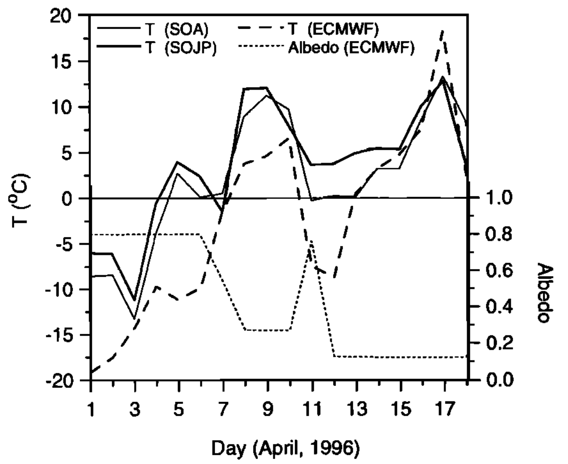

Figure 1. Time series of observed and ECMWF model forecast 2-m temperatures at 0000 UTC for BOREAS southern study area Old Aspen and Old Jack Pine sites, together with model albedo.

2.2. Revised Snow Albedo Scheme

The new snow albedo scheme is simpler than the old one, because it was recognized that the current ECMWF forecast model does not have a field for vegetation type, and the single roughness field includes the effect of orography. However, the forest areas can be identified in the model based on their snow-free background albedo (which is a fixed model field, taken from the climatology of *Dorman and Sellers* [1989]). The land points shown shaded in Figure 2(top) are the areas of the globe covered by forest, where the background albedo, α_B, is less than 15%. Figure 2(bottom), from the International Satellite Land Surface Climatology Project (ISLSCP) data set of *Sellers et al.* [1996] also identifies the forest types with dark shading. The correspondence between the two figures is sufficiently close that we used background albedo to identify forests, rather than introduce another constant field for vegetation type in the model. An albedo for the snow-covered part of the grid box, α_S, is now defined as

$$\alpha_S = \min(a_2, \max(a_1, a_1 + c_1(\alpha_B - b_1))) \quad (1)$$

$$a_1=0.2, \quad a_2=0.7, \quad b_1=0.13, \quad b_2=0.15, \quad c_1=(a_1-a_2)/(b_1-b_2)$$

Equation (1) ensures a deep snow albedo of 0.2 for forest-covered areas (background albedo smaller than 0.13), 0.7 for forest-free areas (background albedo larger than 0.15), and a linear relationship linking the two. The Appendix gives more details. Note the reduction, from 0.8 to 0.7, between the previous and the new maximum albedo value over snow. The previous value (0.8) is representative of fresh clean snow conditions; the new slightly lower value (0.7) was introduced as a compromise value, because the simple parametrization does not take into account the effects of snow ageing, which reduces albedo.

Figure 3 compares the old (labeled control) and the new model albedo in the first day (March 31, 1996) of the two forecasts with triangular truncation T106. The new albedo values are greatly reduced over the areas identified as forests in Figure 2(top). Typical new values in this areas are 0.2, compared with old values in excess of 0.7.

To summarize, the old model albedo over snow-covered areas was ineffective in its way of distinguishing forest from nonforest areas, since beyond a relatively small snow depth, the albedo is of the order of 0.7-0.8. The new simple treatment for snow albedo, described above, distinguishes the albedo over forests from the albedo over lower vegetation. The forested areas, defined as areas of small background albedo, have a final model deep snow albedo of 0.2, while over the nonforested areas, the corresponding limit is 0.7.

2.3. Operational Model Cycles

There are three model versions relevant to this paper. The operational model in winter and spring of 1996 was cycle 14R3, and our ensembles of forecasts are initialized with these operational analyses. As well as the forest albedo error, 14R3 had a substantial cold winter temperature bias. This was corrected in cycle 15R5 [*Viterbo et al.*, 1999], which introduced soil freezing and changes to the stable boundary layer, as well as increased the coupling between soil and atmosphere. Cycle 15R5 became operational in September 1996, and it is used as the control forecast model for our ensembles, as it contains the old albedo scheme. The model cycle 15R6 contains, in addition, the modifications to the snow albedo discussed in section 2.2: it became the operational model in December 1996, following the set of experiments described here.

3. Impact of Albedo Change on Forecasts

The impact on forecasts is largest in the spring period, when snow lies on the ground and the incoming solar radiation is large. This section describes the results from a set of forty 10-day

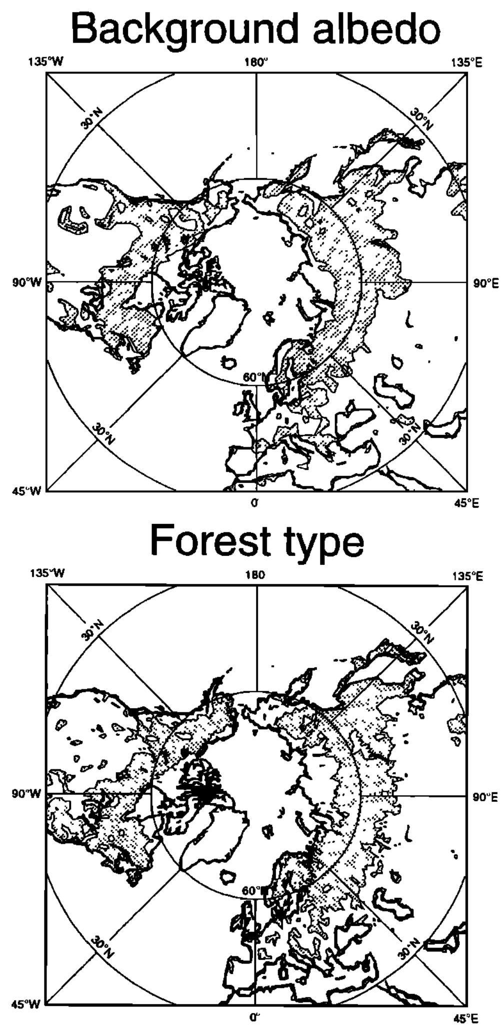

Figure 2. (top) Background albedo. Shaded values over land represent values smaller than 0.15. (bottom) ISLSCP initiative 1 vegetation type. Shaded values over land represent all types of forest.

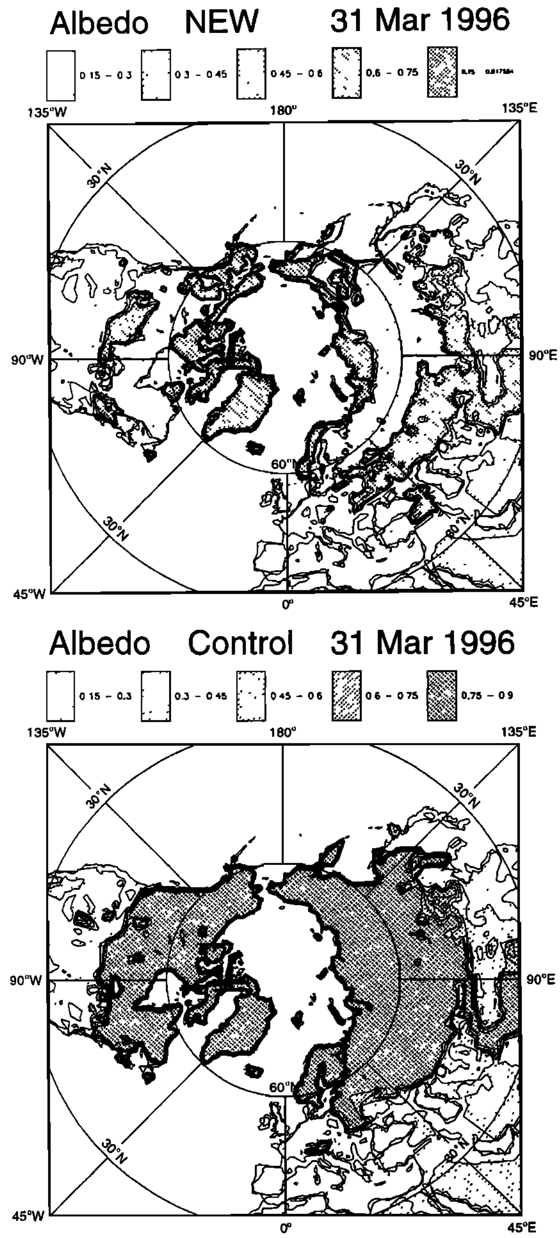

Figure 3. Forecast albedo for March 31, 1996, for new albedo model (top) and old albedo model (bottom).

forecasts with resolution T106L31 (triangular truncation of T106 and 31 levels in the vertical), which were run with initial conditions from 1200 UTC every third day between February 2 and May 29, 1996, for cycle 15R5 (designated control), and the new albedo scheme 15R6 (designated new). These forecasts are initialized with the available operational analysis (14R3), which has a substantial cold soil and surface temperature bias. In section 3.2 we show the additional beneficial impact of correcting this soil temperature error.

3.1. The 2-m Temperature Errors

Figure 4 shows the verification of 2-m temperature for the eleven 60-hour forecasts (corresponding to 0000 UTC) with initial dates between March 15 and April 14, 1996, over the northern part of the North American continent. The top panel is the 15R5 control forecast, where the numbers show that the mean temperature errors are of the order of -10 K. The middle panel is with the new albedo scheme, and the bottom panel shows the difference. Over the Canadian boreal forest the forecast error is reduced from -9 to -12 K to around -2 to -3 K. Most of the temperature errors in the new albedo panel lie within the interval -2 to 2 K, although a few points around the Hudson Bay are now too warm. The 72-hour forecasts over Asia and northern Europe (not shown) show very similar benefits, with a large improvement in Asia, where the warming at the surface exceeds 10 K over a very large area. Statistics from the above three areas are summarized in Table 1.

The control forecasts in the whole ensemble were 15R5, starting from the (cold) operational soil temperatures, given by the 14R3 analysis. Although 15R5 includes soil water freezing and changes to the stable layer parameterization, the effect of these changes is small in these short-term forecasts. Consequently, although the new snow albedo reduces the cold bias, it is not completely removed.

3.2. Impact of Soil Temperature Error

To assess separately the impact of the cold soil temperature error in the analysis, we ran three forecasts with the initial date April 1, 1996, with the results summarized in Table 2. Cycle 14R3 is the operational forecast, and forecasts were initialized with the 14R3 operational analysis at 1200 UTC. The forecasts correspond to 1200 UTC over Europe and Asia, and 1800 UTC over North America.

In the development of 15R5 a long "soil temperature assimilation" run was made [*Viterbo et al.*, 1999] for the full winter of 1996 to obtain corrected soil temperatures. We inserted these soil temperatures into the analysis for April 1, 1996, and made the other two forecasts in Table 2, one labeled 15R5 (T_{soil} corrected) and the third one, with the snow modifications, 15R6 (T_{soil} corrected). Results in the table are an illustration of the true separate impact in short-term forecasts of the snow albedo changes between cycle 15R5 and 15R6. In both bias and standard deviation, there is a gradual improvement from 14R3 to 15R6, so that with the new snow albedo, the systematic cold bias has been removed. It is worth noting that the cycle 15R5 modifications to the physics (frozen soil and stable boundary layer) have their maximum impact in winter, when the solar forcing is small, while the albedo modifications described here have their largest impact in the spring season.

3.3. Verification Scores

Figure 5 shows the mean objective scores for the 20 forecasts (controls 15R5 and 15R6 with the new snow albedo) with initial dates in March and April for the northern hemisphere (top) and an east Asian region (bottom). The positive impact on the 850 hPa temperature is global in scale and largest over eastern Asia. The albedo change reduces the lower tropospheric temperature bias shown in the right-hand panels (and with this also reduces the root-mean-square error), as well as benefitting the anomaly correlation scores shown on the left. Consequently, the geopotential height bias (not shown) is reduced. The improved temperature structure over the continents has positive effects downstream (see Figure 7 in section 4), evident from better scores over North Pacific and North Atlantic (not shown).

Figure 6 shows a time series of northern hemisphere 850 mbar temperature scores for day 5 forecasts from early February to late May. The impact is clearly at its maximum in March and April, fading away in May. Almost every single forecast with the new snow albedo is better than the control with the old albedo scheme. Scatterplots of forecasts for days 1, 3, 5, and 7 for all northern hemisphere continental areas display improvement in almost every forecast (not shown).

4. Improvement of Mean Thermal State in Long Integrations

An ensemble of nine members of 120-day forecasts at resolution T63L31 was run with initial dates between January 30 and February

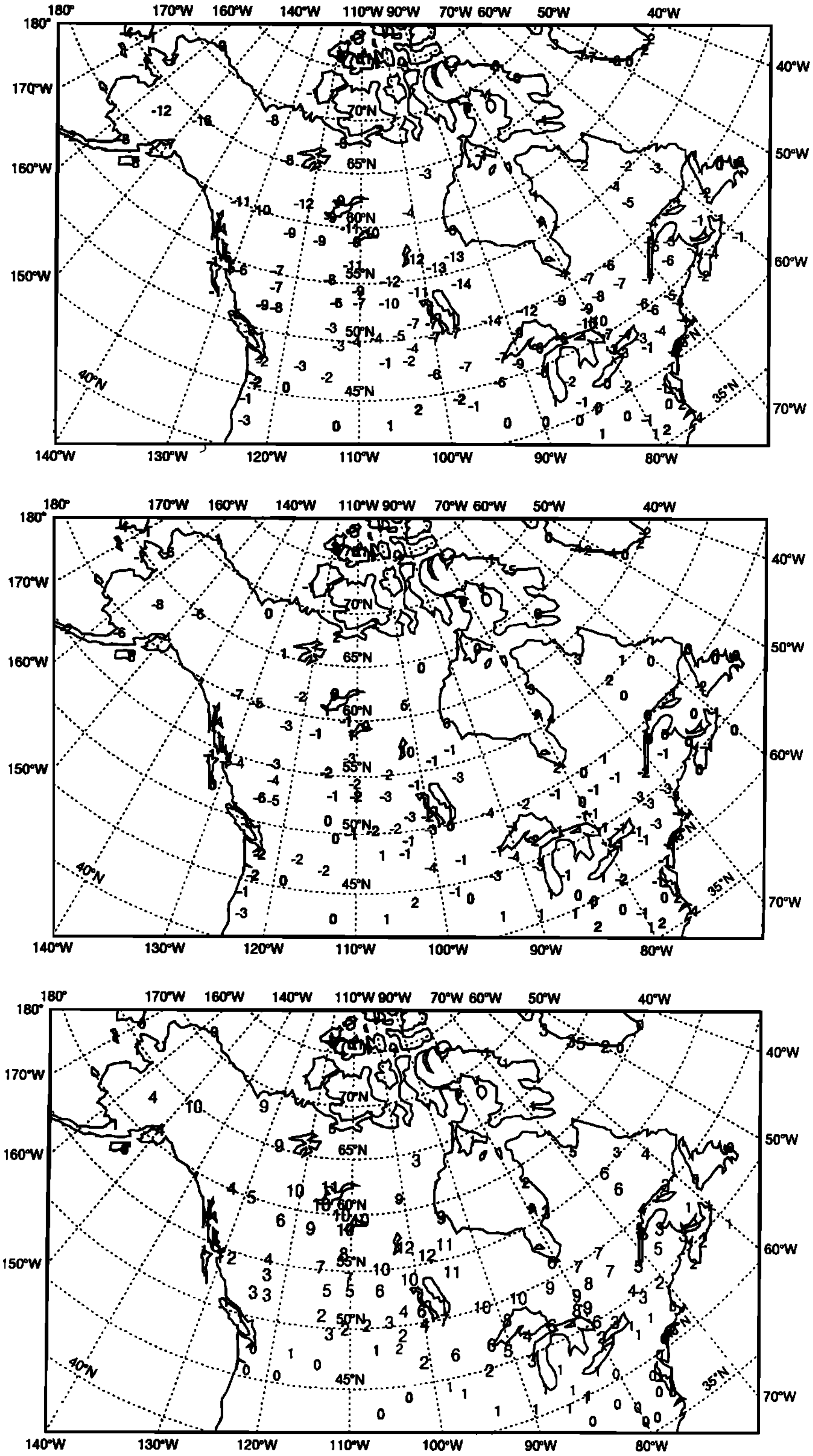

Figure 4. Verification of 2 m temperature over North America, for the 11 T106L31 forecasts with initial dates between March 15 and April 14, 1996. (top) Control 15R5; (middle) new snow albedo 15R6; (bottom) difference new-control.

7, 1996. The mean difference between new and old albedo schemes is shown for March-April-May in Figure 7. The bottom panel shows the 850 mbar temperature difference with contours of 1 K. A large warming of more than 4 K over northeastern Asia and more than 2 K in Canada can be seen; the impact is significant at the 95% level. The top panel shows the 500 hPa geopotential difference (contours in 10 dam), where there are corresponding local impacts over the continents, significant at the 95% level. Perhaps more surprising is

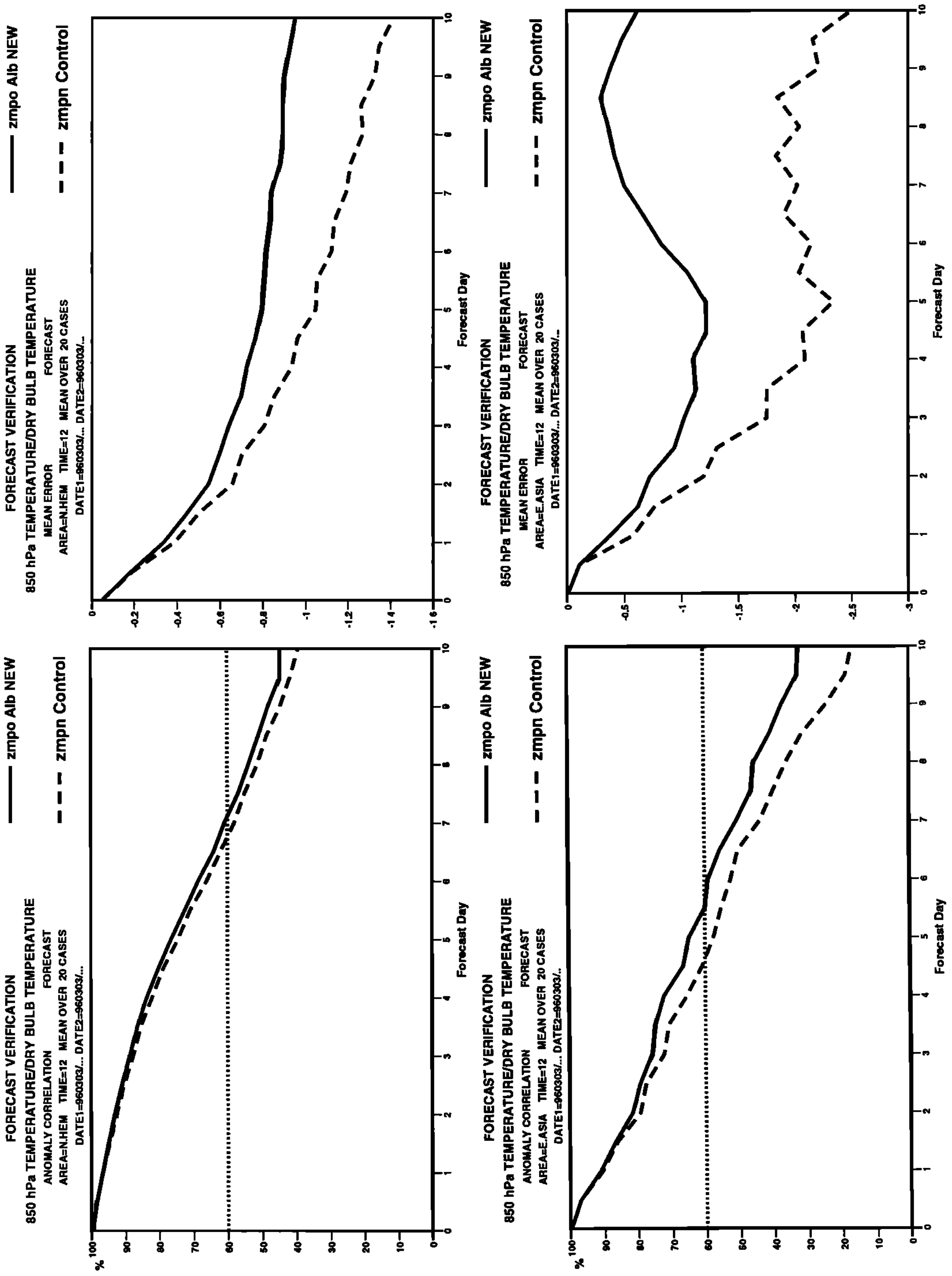

Figure 5. Mean objective scores for 850 hPa temperature for the 20 T106 forecasts with initial dates between March 3 and April 29, 1996. For each area the anomaly correlation (left) and bias (right) are shown. (top) Northern Hemisphere and (bottom) eastern Asia.

Table 1. Statistics on the Comparison of 2-m Temperature Against Observations, for All Forecasts Verifying between March 15 and April 14, 1996.

	Bias	Standard Deviation
	Northern Europe 72 hours	
15R5 (control)	-4.16	5.80
15R6 (new)	-2.25	3.95
	Asia 72hours	
15R5 (control)	-7.63	6.57
15R6 (new)	-2.66	4.03
	North America 60 hours	
15R5 (control)	-3.59	5.74
15R6 (new)	-0.69	3.86

All forecasts are initialized with the 14R3 operational analysis.

Table 2 Statistics on the Comparison of 2-m Temperature Against Observations initialized on April 1, 1996

	Bias	Standard Deviation
	Northern Europe, 72 hour	
14R3	-4.24	4.51
15R5 (T_{soil} corrected)	-0.71	4.21
15R6 (T_{soil} corrected)	0.25	3.61
	Asia 72 hours	
14R3	-9.02	7.17
15R5 (T_{soil} corrected)	-4.38	6.09
15R6 (T_{soil} corrected)	-0.74	3.37
	North America 78 hours	
14R3	-5.54	7.78
15R5 (T_{soil} corrected)	-2.43	6.57
15R6 (T_{soil} corrected)	-0.21	4.85

to see the impact over the western Pacific at 500 hPa, where a more pronounced trough significantly reduces the model systematic error for this region (not shown).

Figure 8 differences the zonal mean temperature error of the new and control albedo forecasts for the last month (May) of the ensemble of 120-day integrations. The effect of the new snow albedo over the boreal forests is to produce a large warming from 45° to 80°N from the surface up to 600 hPa, largely eliminating the model cold bias in the lower troposphere at 60°N. This shows that the impact of the surface albedo change extends through a deep tropospheric layer. There is a moistening of up to 0.5 gkg^{-1} in the same areas (not shown); while the impact on the zonal mean zonal wind is small (not shown).

5. Discussion and Conclusions

A change in the model snow albedo and its impact has been presented. While the previous snow albedo was of the order of 0.7-0.8 for relatively small snow depths, the new formulation has a deep snow albedo of 0.2 in boreal forest areas and 0.7 in forest-free areas. Results presented show a very large positive impact on the forecast 2-m temperatures in spring and a reduction of the lower tropospheric cold bias in spring. The impact on forecasts in the northern hemisphere is large and positive from February to May and negligible for all other areas and seasons.

The new snow formulation was included in cycle 15R6, which became operational in December 1996. Plate 1 compares (with the same color contours) the average March-April 850 mbar 5-day forecast temperature errors in the operational model for 1996 and 1997. At high northern latitudes the cold bias in spring 1996 at 850 mbar grows rapidly (within a few days), and at 5 days, it is as large as -6 K over eastern Russia. There was also a positive temperature bias over China. In spring 1997, with the new snow albedo scheme, the cold bias over the boreal forests has been almost eliminated, although a residual cold bias can now be seen near 40°N over Asia. These operational forecasts are for two different years, but it is clear that the change to the snow albedo scheme for the boreal forests has greatly reduced the model systematic temperature error in spring in the northern hemisphere.

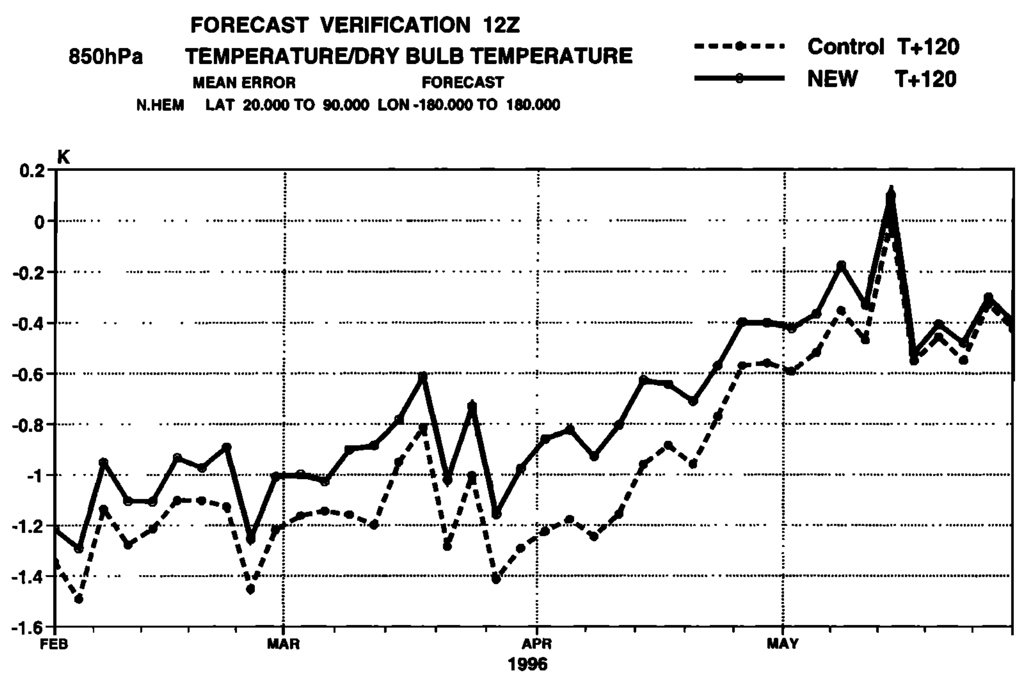

Figure 6. Time series of bias of 850 hPa Northern Hemisphere temperatures for the forecasts with initial dates between February 2 and May 29, 1996.

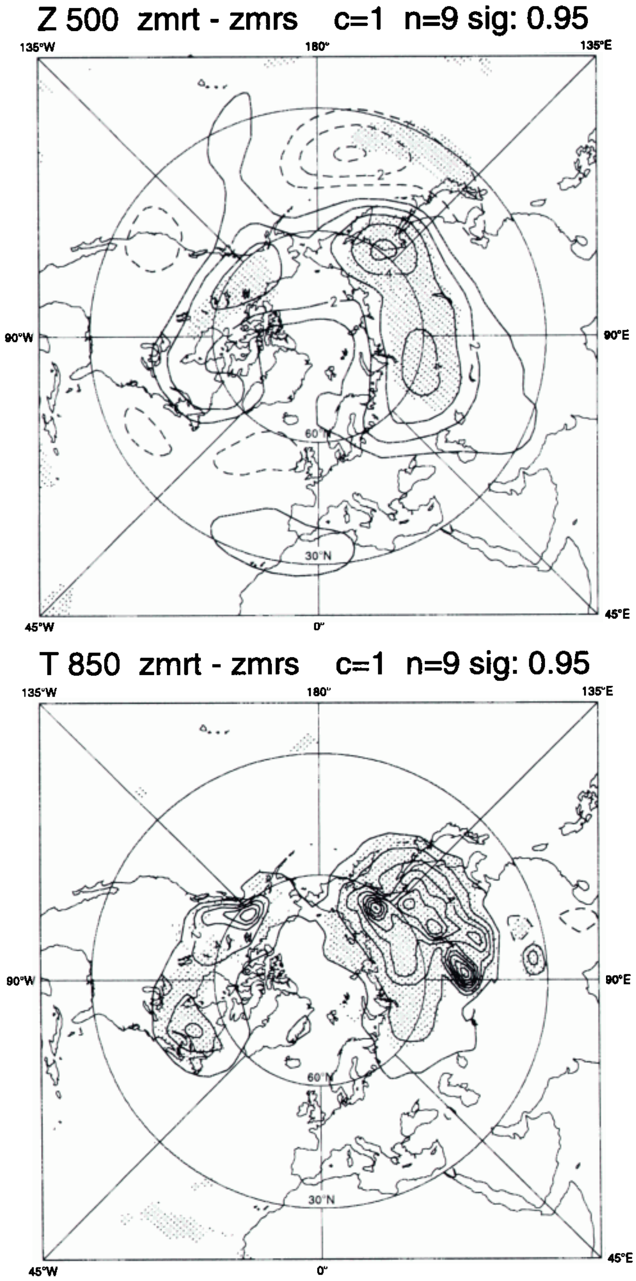

Figure 7. March-April-May mean difference of 850 hPa temperature (top) and 500 hPa geopotential for new 15R6-control 15R5 for an ensemble of nine T63L31 integrations, starting near the beginning of February. Shaded areas in the difference plot correspond to significant differences at 95% level.

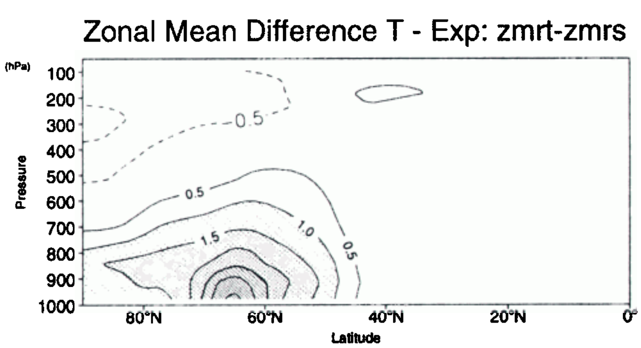

Figure 8. Zonal mean temperature difference (new-control) for Northern Hemisphere for the last month (May) for the ensemble of nine T63L31 120-day integrations.

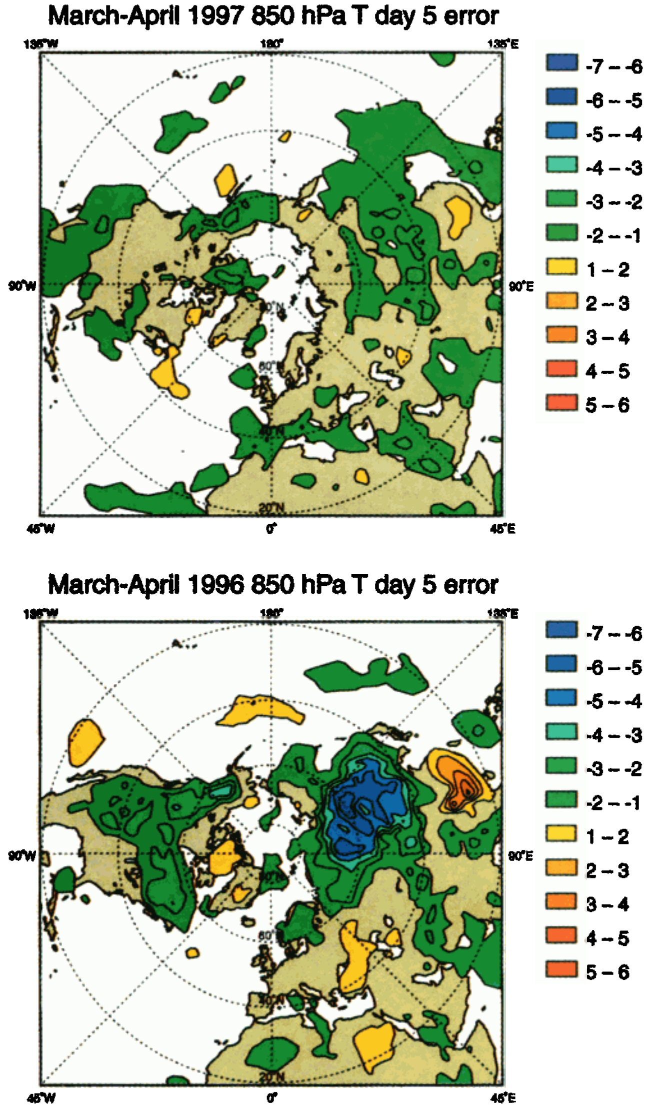

Plate 1. Comparison of the average 5-day forecast temperature errors at 850 mbar in the ECMWF operational model for March-April 1996 and 1997.

Future changes in the snow formulation, including a better vegetation distribution, a better handling of melting, and an age-dependent snow albedo and density should further improve on these results. Improvements are also needed in the handling of the snow evaporation, which is now overestimated for the boreal forest regions after this albedo change.

Appendix: Two Model Albedo Schemes

In the operational model prior to December 1996, the snow albedo was derived from a fairly complex series of computations, involving background albedo, snow depth, roughness length, vegetation fraction, surface temperature, and interception reservoir contents. Although such a scheme has, in principle, a sound conceptual basis, the model lacks key parameter fields: it does not have a vegetation map, nor a separate vegetation roughness length (the roughness length for momentum includes an orographic component, which is unrelated to vegetation masking). When the intermediate results of this computation were carefully checked in typical winter and spring situations, it was clear that the end result was unsatisfactory. First an estimate of the fraction of the vegetation covered by snow was made, based on the roughness length for momentum. However, over the boreal forest the implicit masking of snow by vegetation (in the model) is small. An effective snow covered-fraction of the grid box is also calculated, based on the snow water equivalent depth, but in winter for the boreal forest, this value in the model is very rarely different from 1. The albedo of the snow part of the grid box increases from a minimum of 0.4 at soil temperatures of 0°C to a maximum of 0.8 below -5°C. Given the large cold bias in the model (before the 1996-1997 winter), this value is most of the time around 0.8. A first estimate of the grid box albedo is made by combining the background albedo with the snow albedo, based on the effective fraction defined above. Finally, this estimate can be further increased in the presence of ice dew, which brings the albedo up to 0.8 in some areas that were still below this value. The end result of all the above computations is an albedo in the presence of snow that is rarely outside of the 0.7-0.8 range, as shown earlier in Figure 3(bottom).

In the new scheme, an albedo for the snow-covered part of the grid box, αS (defined by equation (1) in section 2.2), ensures a deep snow albedo of 0.2 for forest-covered areas (background albedo smaller than 0.13), 0.7 for forest-free areas (background albedo larger than 0.15), and a linear relationship linking the two. The fraction of the grid box covered by snow is given by

$$C_S = \min(1, Sn/Sn_c) \quad Sn_c = 0.015 \tag{2}$$

where Snc is the snow amount in meters of equivalent water. A first estimate of the grid box albedo α^* is given as a linear combination of eq. (1) and the background albedo,

$$\alpha_* = C_S\alpha_s + (1 - C_S)\alpha_B \tag{3}$$

To obtain the final forecast albedo αF, an ice dew correction is added for forest free areas

$$\alpha_F = \max(\alpha_D, \alpha_*) \tag{4}$$

$$\alpha_D = 0.4 f_1 f_2 C_l,$$

$$f_1 = \min(1, \max(0, \frac{\alpha_B - b_1}{b_1 - b_2})), \; f_2 = \min(1, \max(0, \frac{T_0 - T_s}{5}))$$

In eq. (4), Ts and T0 represent, respectively, the soil temperature and the freezing temperature, while Cl is the fraction of the grid box covered by the interception reservoir, defined by Viterbo and Beljaars [1995].

Acknowledgments. Alan Betts was supported by NASA under grant NAG5-7377 and the National Science Foundation under grant ATM95-05018. ECMWF provided travel support.

References

Betts, A.K., and J.H. Ball, Albedo over the boreal forest, *J. Geophys. Res.*, *102*, 28,901-28,913, 1997.

Betts, A.K., P. Viterbo, A.C.M. Beljaars, H.-L. Pan, S.-Y. Hong, M. L. Goulden, and S.C. Wofsy, Evaluation of the land-surface interaction in the ECMWF and NCEP/NCAR reanalyses over grassland (FIFE) and boreal forest (BOREAS), *J. Geophys. Res.*, *103*, 23,079-23,085, 1998.

Dorman, J.L., and P.J. Sellers, A global climatology of albedo, roughness length and stomatal resistance for atmospheric general circulation models as represented by the Simple Biosphere Model (SiB), *J. Appl. Meteorol.*, *28*, 833-855, 1989.

Harding, R. J., and J. W. Pomeroy, The energy balance of the winter boreal landscape, *J. Clim.*, *9*, 2778-2787, 1996.

Laine, V., and M. Heikinheimo, Estimation of surface albedo from NOAA AVHRR data in high latitudes, *Tellus, Ser. A*, *48*, 424-441, 1996.

Pomeroy, K. W., and K. Dion, Winter radiation extinction and reflection in a boreal pine canopy: measurements and modeling, *Hydrolog. Processes*, *10*, 1591-1608, 1996.

Robinson, D.A., and G. Kukla, Albedo of a dissipating snow cover, *J. Clim. Appl. Meteorol.*, *24*, 402-411, 1984.

Robinson, D.A., and G. Kukla, Maximum surface albedo of seasonally snow-covered lands in the Northern Hemisphere, *J. Clim. Appl. Meteorol.*, *24*, 402-411, 1985.

Sellers, P.J., et al., The ISLSCP initiative I-global data sets: Surface boundary conditions and atmospheric forcings for land-atmosphere models, *Bull. Am. Meteorol. Soc.*, *77*, 1987-2005, 1996.

Sellers, P.J. et al., BOREAS in 1997: Experiment overview, scientific results, and future directions, *J. Geophys. Res.*, *102*, 28, 731-28, 769, 1997.

Viterbo, P., and A.C.M. Beljaars, An improved land-surface parameterization in the ECMWF model and its validation, *J. Clim.*, *8*, 2716-2748, 1995.

Viterbo, P., A.C.M. Beljaars, J.-F. Mahfouf, and J. Teixeira, Soil moisture freezing and its interaction with the boundary layer, *Q. J. R. Meteorol. Soc.*, *124*, in press, 1999.

A. K. Betts, 58 Hendee Lane, Pittsford, VT 05763. (E-mail: akbetts@aol.com)

P. Viterbo, ECMWF, Shinfield Park, Reading, RG2 9AX, England. (E-mail: pav@ecmwf.int)

(Received August, 8, 1998; revised October 20, 1998; accepted October 27, 1998.)